Letter

# Ultrafast element- and depth-resolved magnetization dynamics probed by transverse magneto-optical Kerr effect spectroscopy in the soft x-ray range

Martin Hennecke,[1,*] Daniel Schick,[1,†] Themistoklis Sidiropoulos,[1] Felix Willems,[1] Anke Heilmann,[1] Martin Bock,[1] Lutz Ehrentraut,[1] Dieter Engel,[1] Piet Hessing,[1] Bastian Pfau,[1] Martin Schmidbauer,[2] Andreas Furchner,[3,4] Matthias Schnuerer,[1] Clemens von Korff Schmising,[1] and Stefan Eisebitt[1,5]

[1]*Max-Born-Institut für Nichtlineare Optik und Kurzzeitspektroskopie, Max-Born-Straße 2A, 12489 Berlin, Germany*
[2]*Leibniz-Institut für Kristallzüchtung, Max-Born-Straße 2, 12489 Berlin, Germany*
[3]*Helmholtz-Zentrum Berlin für Materialien und Energie, Division Energy and Information, Schwarzschildstraße 8, 12489 Berlin, Germany*
[4]*Department Berlin, Leibniz-Institut für Analytische Wissenschaften-ISAS-e.V., Schwarzschildstraße 8, 12489 Berlin, Germany*
[5]*Institut für Optik und Atomare Physik, Technische Universität Berlin, Straße des 17, Juni 135, 10623 Berlin, Germany*

(Received 12 October 2021; revised 13 May 2022; accepted 17 May 2022; published 21 June 2022)

We report on time- and angle-resolved transverse magneto-optical Kerr effect spectroscopy in the soft x-ray range that, by analysis via polarization-dependent magnetic scattering simulations, allows us to determine the spatiotemporal and element-specific evolution of femtosecond laser-induced spin dynamics in nanostructured magnetic materials. In a ferrimagnetic GdFe thin-film system, we correlate a reshaping spectrum of the magneto-optical Kerr signal to depth-dependent magnetization dynamics and disentangle contributions due to nonequilibrium electron transport and nanoscale heat diffusion on their intrinsic timescales. Our Letter provides a quantitative insight into light-driven spin dynamics occurring at buried interfaces of complex magnetic heterostructures, which can be tailored and functionalized for future optospintronic devices.

DOI: 10.1103/PhysRevResearch.4.L022062

The recent advances in ultrafast magnetism research [1,2] have made it possible to develop the understanding of laser-driven spin dynamics from microscopic processes towards macroscopic functionality in complex systems including charge and spin transport [3–7] as well as interactions with spatially extended quasiparticles, such as phonons and magnons [8–15]. These findings are exploited in today's optospintronics where magnetic order is optically controlled in buried layers and across multiple interfaces of tailored magnetic nanostructures. The combination of spatiotemporal spin manipulation and structure design on the nanoscale is highly relevant for novel ultrafast and energy-efficient information technology [16], thermoelectrics [17], and terahertz emitters [18]. Whereas common optical and transport-based magnetometry only provides an indirect access to the spatial dependence of the relevant nonlocal spin dynamics, ultrafast resonant magnetic soft x-ray scattering [19] is a unique technique, which combines magnetic contrast with element selectivity and nanoscale depth resolution, utilizing the short wavelength of the radiation with access to core-level resonances. This has been exploited in first steps towards ultrafast magnetization depth profiling at large scale facilities [20,21], however, so far without being able to provide a quantitative analysis of the spatially inhomogeneous evolution of the magnetization with subpicosecond temporal resolution. One challenge in order to exploit resonant magnetic scattering for nanoscale magnetization profiling is related to the complex interplay of angle- and/or photon energy-dependent absorption, refraction, interlayer reflections, and interference effects. To that end, it is inevitable to compare the resulting complex scattering patterns with magnetic scattering simulations [22,23] relying on carefully determined atomic and magnetic form factors especially for photon energies in close vicinity to core-to-valence-band transitions. Continuous progress in laser-driven table-top light sources based on high-harmonic generation (HHG) has started to provide access to the relevant soft x-ray regime—for a long time the exclusive domain of large-scale facilities, such as synchrotrons and free-electron lasers. In particular, HHG with control over the light polarization [24–27] has enabled laboratory-based experiments on magnetization dynamics with temporal resolutions down to the femtosecond [28–32] or even attosecond regime [33]. Above all, the broadband properties of HHG radiation allow measurements of large spectral regions in a single acquisition, providing simultaneous access to characteristic spectral features at their intrinsic timescale.

In this Letter, we study the spatial evolution of the ultrafast magnetization dynamics in a ferrimagnetic Ta/GdFe/Pt nanolayer system; a model system exhibiting intriguing magnetic functionality, such as single shot all-optical switching [34,35] and self-induced spin-orbit torques [36,37], both relevant for potential spintronics applications. We conduct femtosecond time-resolved and angle-resolved transverse

*hennecke@mbi-berlin.de
†schick@mbi-berlin.de

*Published by the American Physical Society under the terms of the Creative Commons Attribution 4.0 International license. Further distribution of this work must maintain attribution to the author(s) and the published article's title, journal citation, and DOI.*

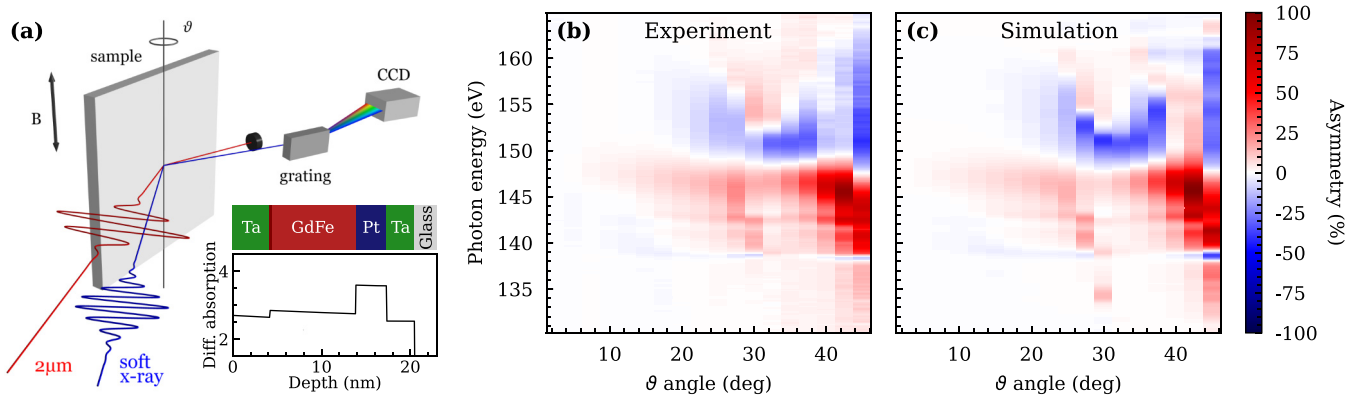


FIG. 1. (a) Schematic of the $\vartheta$-$2\vartheta$ spectroscopy setup used for the angle- and time-resolved experiments. The inset shows the depth-dependent differential absorption of the 2.1-$\mu$m pump pulse (incident from the left side onto the Ta layer) that drives the magnetization dynamics. (b) Static angle-resolved TMOKE asymmetry spectra (color scale) of the studied GdFe sample measured by soft x-ray pulses in the photon energy range across the Gd $N_{5,4}$ resonance. (c) Simulation of the static angle-resolved TMOKE asymmetry spectra fitted to the experimental data in panel (b).

magneto-optical Kerr effect (TMOKE) spectroscopy at the Gd $N_{5,4}$ resonance around 150-eV photon energy, selectively probing the magnetization of the Gd sublattice. Our analysis reveals significant differences in the ultrafast evolution of the TMOKE asymmetry for different photon energies. By comparison to polarization-dependent magnetic scattering simulations, we can quantitatively relate these spectral changes to transient, depth-dependent demagnetization and remagnetization profiles within the GdFe layer after photoexcitation. Analysis of the evolving magnetization depth profiles allows us to disentangle femtosecond dynamics dominated by nonequilibrium electron transport ($\leqslant 100$ fs) and nanoscale heat diffusion on a picosecond timescale ($\geqslant 1$ ps). Based on our experimental data, we, hence, rule out significant contributions due to femtosecond nonlocal spin transport phenomena, but observe the emergence of a magnetization gradient within GdFe within approximately 1 ps, induced by heat injection at the interface with the buried seed layer. Our results emphasize the importance of a careful analysis of magnetic scattering data as inhomogeneous spin dynamics in layered magnetic systems results in a complicated spectral dependence of the TMOKE observable. In turn, this allows us to disentangle local and nonlocal processes on ultrafast timescales. Importantly, our findings directly correlate experimental observables with functionality in nanoscale device structures, e.g., controlled by charge or spin currents as well as nanoscale heat transfer.

The TMOKE measurements are carried out employing a combined $\vartheta$-$2\vartheta$ reflectometry and spectroscopy setup as schematically illustrated in Fig. 1(a). The probing soft x rays are provided by a laboratory HHG-based light source. The HHG process is driven by a high average power (29-W) optical parametric chirped-pulse amplifier system emitting in the midinfrared (MIR) spectral range at 2.1-$\mu$m center wavelength with 27-fs full width at half maximum (FWHM) pulse duration. The source delivers $\leqslant$27-fs FWHM soft x-ray pulses at a 10-kHz repetition rate over a broad and continuous spectrum of which we use the 100–200-eV region in this experiment [38]. A fraction of the MIR beam is separately guided over a variable delay line, providing synchronized pump pulses for inducing ultrafast magnetization dynamics in the sample in time-resolved pump-probe experiments. Both pulses are $p$ polarized and focused onto the sample almost collinearly, facilitating a temporal resolution of $\approx$50 fs. The soft x-ray pulses are incident under a glancing angle $\vartheta$ on the sample and reflected into the spectrometer placed at $2\vartheta$ with respect to the soft x-ray beam axis. The spectrum is horizontally dispersed and focused onto a CCD camera upon reflection by a variable line spacing grating, achieving a photon energy resolution down to 0.5 eV (for more experimental details, see the Supplemental Material [39]).

The sample investigated is an amorphous ferrimagnetic $Gd_{24}Fe_{76}$ alloy with in-plane magnetic anisotropy deposited by magnetron sputtering on a 400-$\mu$m thick glass substrate, seeded by a Pt layer and capped with Ta to prevent oxidation of the ferrimagnetic layer. All measurements were carried out at room temperature ($\approx$300 K), which is below the ferrimagnetic compensation temperature of the studied GdFe layer [40]. Static angle-resolved TMOKE spectra of the sample measured in the photon energy range across the Gd $N_{5,4}$ resonance for angles of incidence ranging from $\vartheta = 2.5^\circ$ up to $45^\circ$ are shown in Fig. 1(b). The magnetic asymmetry is calculated from two spectra recorded for opposite directions of a saturating in-plane magnetic field applied perpendicular to the $p$-polarization axis of the soft x-ray pulses. The experimental data are reproduced with high accuracy by the magnetic scattering simulations shown in Fig. 1(c) [23,41]. The simulations include the photon energy-dependent reflectivity of the $p$-polarized soft x-rays resulting from the element-specific atomic and magnetic form factors, taking into account both the structural properties of the individual layers, i.e., thickness, density, and roughness, as well as the magnetic moments in the GdFe layer. By numerically calculating the polarization-dependent wave propagation for each angle of incidence and photon energy, the varying absorption, refraction, and probing depth in the vicinity of the atomic resonance is taken into account for both magnetization states of the sample. Simulating the $\vartheta$-$2\vartheta$ spectroscopy data, thus, allows us to fit both the structural parameters of the sample as well as the GdFe layer's equilibrium

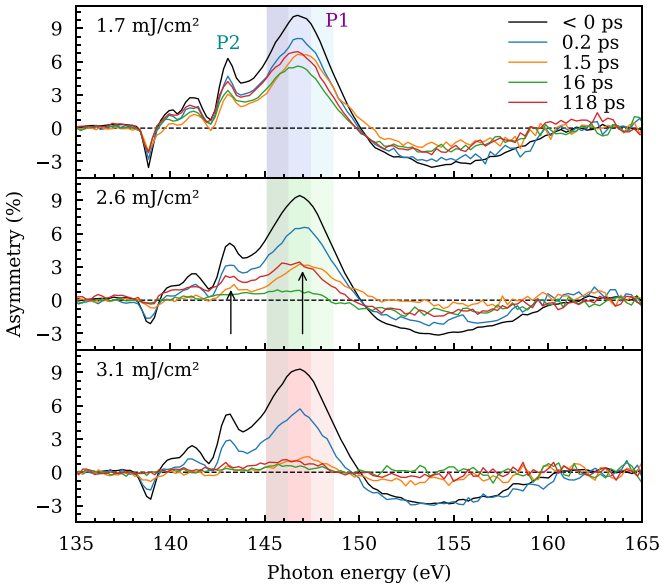


FIG. 2. Transient TMOKE asymmetry spectra at $\vartheta = 20^\circ$ as a function of incident excitation fluence and pump-probe delay. Each plot shows the equilibrium state (black) as well as a series of transient spectra (colored) recorded at different delays after excitation. The shaded areas indicate different photon energy intervals for each fluence (blue, green, and red) over which the asymmetry was integrated to obtain the time traces shown in Fig. 3(b). The arrows mark the time evolution of the main (P1) and neighboring (P2) asymmetry peaks.

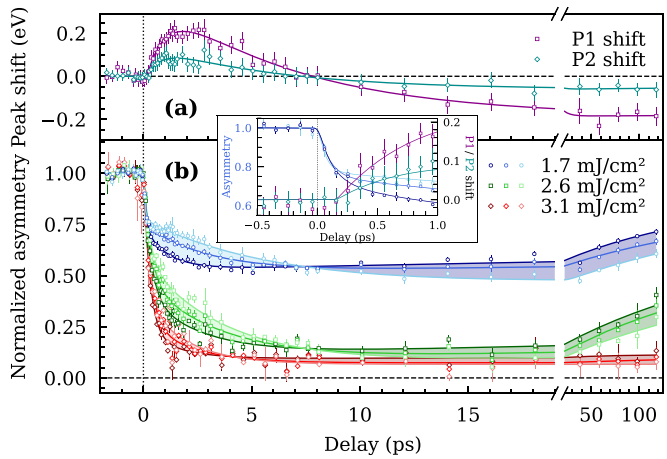


FIG. 3. (a) Transient shift of the main (P1) and its neighboring (P2) asymmetry peak upon 1.7 mJ/cm$^2$ excitation. (b) Integrated asymmetry as a function of excitation fluence and pump-probe delay. The colored data points for each fluence result from integrating over the accordingly colored photon energy intervals shown in Fig. 2. The inset compares the demagnetization dynamics and peak shifts during the first picosecond after excitation.

magnetization component perpendicular to the $p$-polarization axis of the probing soft x-ray pulses (see the Supplemental Material [39] for more details about the simulations and fits). The resulting sample composition (thickness in nanometers) is Ta(4.2)/$Gd_{24}Fe_{76}$(9.7)/Pt(3.5)/Ta(3.2)/glass. Mapping the magnetization profile within the GdFe layer with 0.2-nm resolution, the fit converges for a static magnetization profile that slightly decreases towards the interfaces with both the Ta cap and the Pt seed layers. The high agreement between the experimental data and the simulation shown in Fig. 1 proves the ability to determine quantitative magnetization depth profiles and structural parameters with subnanometer resolution.

Time-resolved pump-probe studies were carried out at a soft x-ray probing angle of $\vartheta = 20^\circ$. The evolution of the asymmetry measured in the photon energy range across the Gd $N_{5,4}$ resonance is shown in Fig. 2 for selected delays and excitation fluences. Following the incidence of the pump pulse at 0 ps, the magnitude of the magnetic asymmetry decreases with respect to the unexcited equilibrium state due to the laser-induced demagnetization of the GdFe layer. Comparison of the asymmetry spectra for different time delays after excitation further reveals significant changes in their spectral shape, including a shift of the main peak (P1); first towards higher and later towards lower photon energies with respect to the equilibrium position at $< 0$ ps. In addition, the relative pump-induced amplitude changes also show a pronounced spectral dependence. This can be seen particularly well for an incident fluence of 2.6 mJ/cm$^2$ (center panel of Fig. 2), following the time evolution of the peak amplitudes P1 and P2 at early (1.5-ps) and late (118-ps) times. The observed shift and photon energy dependence is further analyzed in Fig. 3. Panel (a) shows the transient relative shifts of the asymmetry peaks P1 and P2 upon 1.7-mJ/cm$^2$ excitation, obtained from a Gaussian multipeak fit of the time-resolved spectra. Significantly different shifts of the two peaks can be observed which after 1 to 2 ps approach their maxima of $\approx$200 meV and $\approx$100 meV, respectively, stretching the spectrum on the photon energy axis. As indicated by the inset, the shifting of peaks starts with a delay of $\approx$200 fs after the initial, ultrafast drop of the femtosecond demagnetization. At later times, a much slower shift towards the opposite direction leads to a sign change after 8 ps and a long-lived shifted state which is still present after 120 ps when the magnetization of the system starts to relax back to its initial state. These effects have a strong impact on the TMOKE observable, when the asymmetry signals are integrated within a finite spectral bandwidth around the asymmetry peak of an element-specific resonance as is usually performed for obtaining magnetization transients as a function of delay time. This is emphasized in Fig. 3(b), which shows the peak-integrated asymmetry as a function of incident excitation fluence obtained by integrating the time-resolved spectra over slightly shifted photon energy intervals as indicated by the shaded areas in Fig. 2. The data are fitted with triple-exponential functions as a guide to the eye. It becomes obvious that the perceived magnetization dynamics of the GdFe layer is highly dependent on the choice of the integration window, resulting in transients that indicate contradicting magnitude and speed of the pump-induced magnetization change [indicated by the filled areas between the time traces shown in Fig. 3(b)]. Our observation shows that the TMOKE asymmetries measured at different photon energies are not proportional to a uniform magnetization averaged over the whole depth of the magnetic layer. This indicates that the asymmetries emerge from different probing volumes as the absorption length strongly varies across the

giant $N_{5,4}$ resonance. The spectral dependence of the pump-induced change, therefore, strongly suggests depth-dependent magnetization dynamics of the GdFe layer. To that end, we have carefully ruled out any nonmagnetic contribution, by finding within our signal-to-noise level no transient change in the reflectivity spectra, which measure the laser-induced change of the average $4f$ electronic state occupation (see the Supplemental Material [39]). This, in turn, implies that the initial ultrafast drop of the localized Gd $4f$ moment is driven by optical excitation of $5d6s$ valence electrons and the very strong intra-atomic exchange coupling between localized $4f$ and itinerant $5d$ moments [42,43].

In order to obtain the transient magnetization profiles of the system, the time-resolved experimental data were fitted by simulated asymmetry spectra, varying only the magnetization distribution within the GdFe layer as a fit parameter whereas keeping the structural parameters fixed that were determined from the previous static angle-resolved measurements. We model the magnetization profile as a second-order polynomial function as the simplest mathematical description reflecting the asymmetric layer structure of our sample with different cap and seed layers, Ta and Pt, respectively. Transient changes in the structure, e.g., due to acoustic deformations, result only in marginal changes in the calculated asymmetry spectra for the range of excitation fluences studied and have been neglected, accordingly. For the sake of clarity and to achieve a better signal-to-noise ratio, the measured asymmetry spectra were averaged over different time intervals, i.e., at early times before the excitation pulse hits the sample and at two later times where the observed shift of the asymmetry peaks is largest in both directions [compare Fig. 3(a)]. The simulation is able to reproduce the observed behavior of the transient TMOKE spectra with high accuracy by assuming a unique magnetization depth profile for each time interval, see Fig. 4. On the contrary, simulations that assume only a homogeneously distributed magnetization profile or a combination of the latter with transient changes in the atomic nonmagnetic form factors predict significant changes and shifts in the nonmagnetic reflectivity spectra (see the Supplemental Material [39]), which, as mentioned before, are not observed in the experiment, or otherwise lead to a significantly worse agreement with the experimental data.

The transient evolution of the magnetization profiles can thereby be understood as follows: Before 0 ps, there is already a slight fluence-dependent decrease in the magnetization with respect to the nonexcited equilibrium state due to static heating of the sample. This is caused by the absorption of the repetitively arriving pump pulses during the pump-probe measurements. After a pump pulse hits the sample, it causes a thermally induced demagnetization within the GdFe layer, which is also fluence-dependent. The comparison of experiment and simulation shows that, within a time interval of 1.4–2.6 ps after excitation, the demagnetization is clearly enhanced towards the interface with the Pt seed layer, i.e., on the side of the GdFe layer *not* facing the laser beam. This observation is in line with a numerical simulation of the depth-dependent absorption profile of the 2.1-$\mu$m pump radiation, predicting the deposited energy density to be largest within the Pt seed layer (see the inset of Fig. 1 and the Supplemental Material [39] for more details). In addition to

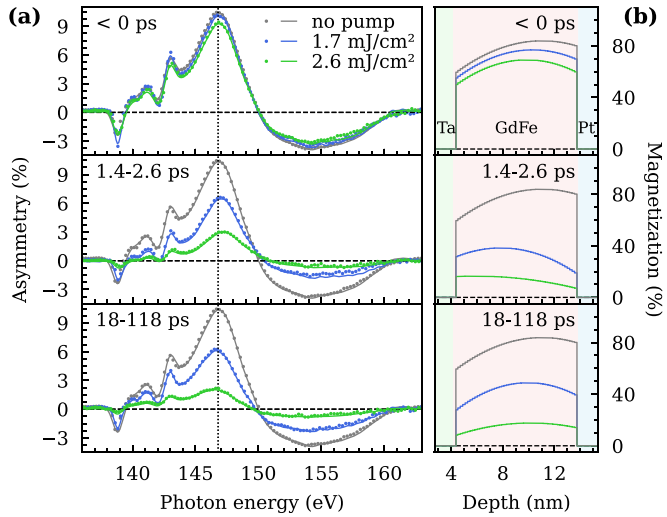


FIG. 4. Determination of the magnetization depth profiles from the time-resolved TMOKE spectroscopy measurements. (a) Recorded transient asymmetry spectra (dots) and fitted simulations (lines) averaged over different time intervals as a function of the incident excitation fluence (black, blue, and green). The simulation was fitted to the experimental data by varying only the magnetization distribution within the GdFe layer. (b) Resulting magnetization depth profiles obtained for the respective excitation fluence and time interval.

the quantitative determination of magnetization depth profiles, our method also reveals that an inhomogeneous change in the magnetization within the GdFe layer must be accompanied by peak shifts in the asymmetry spectra. Based on that we carry out a closer inspection of the transient evolution of the evaluated asymmetry amplitude and peak shift. The decrease of the asymmetry amplitude, as depicted in Fig. 3(b), shows a clear double exponential behavior with a fast ($\approx$100-fs) and a slow ($\approx$1-ps) time constant. These two regimes are commonly referred to as type-II dynamics [44], and their timescales are determined by the equilibration of the spin system with the electronic and phononic subsystems. By comparison to the data in Fig. 3 [panel (a) and inset], we find no sizable asymmetry peak shift evolving in the fast regime during the first hundreds of femtoseconds. This indicates that the initial subpicosecond demagnetization is spatially *homogeneous* within the GdFe layer and that significant contributions due to nonlocal inter- or intralayer transport phenomena, such as superdiffusive spin currents [4], can be excluded. This conclusion again relies on the notion of very strong intra-atomic exchange interaction between localized and itinerant electrons of Gd as required to rationalize the observed ultrafast drop in the Gd $4f$ moment within $<$ 200 fs. Such superdiffusive currents have been shown to lead to significant inhomogeneities in the magnetization profile as well as to interface spin accumulation lasting a few hundreds of femtoseconds after excitation [18,45,46]. In contrast, the significant peak shifts evolving on timescales of 1–3 ps go along with the slower timescale of the type-II dynamics emerging from electron-phonon thermalization. This strongly suggests that due to the layer-dependent laser excitation, phononic heat transfer

from the Pt layer into the GdFe layer on a few picoseconds timescale is the main driver for the evolving inhomogeneous magnetization profile. In contrast, at later times (18–118 ps) when the magnetization starts to relax back to the equilibrium state, we observe a negative peak shift caused by a reversed magnetization profile. This can be rationalized by an opposite thermal gradient evolving due to slow heat dissipation into the glass substrate. Finally, we note that, besides heat diffusion, thermally driven spin currents on picosecond timescales could also contribute to depth-dependent magnetization dynamics, caused, for example, by the spin-dependent Seebeck effect [47,48].

In conclusion, we followed the spatiotemporal and element-selective evolution of magnetization depth profiles in a ferrimagnetic GdFe nanolayer sample by applying ultrafast angle-dependent TMOKE spectroscopy in the soft x-ray spectral range. The comparison of the experimental data to magnetic scattering simulations provides a direct link between the photon energy-dependent temporal evolution of the TMOKE asymmetry and the spatially inhomogeneous magnetization dynamics. With a temporal resolution only limited by the laser pulse durations, our experiment is able to resolve depth- and layer-dependent spin transport from picosecond heat transport in nanostructures down to the ultrashort timescales governed by nonthermal, spin-polarized electron currents. In general, this allows us to distinguish the relevant local and nonlocal processes during ultrafast de- and remagnetization based on their intrinsic temporal and spatial fingerprints.

We thank I. Radu for valuable feedback and discussions. Funding from the German Research Foundation (DFG, Germany) through CRC/TRR 227 project A02 (project ID 328545488) and from the European Union through EFRE Projects 1.8/10 and 1.8/15 is gratefully acknowledged. We thank K. Hinrichs (Leibniz-Institut für Analytische Wissenschaften–ISAS–e.V.) for cooperation via the *Application Laboratory for Infrared Ellipsometry* (funded by European Union Grant No. EFRE 1.8/13), and S. Peters (Sentech Instruments) for his expertise in VIS ellipsometry.

[1] A. Kirilyuk, A. V. Kimel, and T. Rasing, Ultrafast optical manipulation of magnetic order, Rev. Mod. Phys. **82**, 2731 (2010).

[2] K. Carva, P. Baláž, and I. Radu, in *Laser-Induced Ultrafast Magnetic Phenomena*, edited by E. Brück, Handbook of Magnetic Materials Vol. 26 (Elsevier, Amsterdam, 2017), Chap. 2, pp. 291–463.

[3] G. Malinowski, F. Dalla Longa, J. H. H. Rietjens, P. V. Paluskar, R. Huijink, H. J. M. Swagten, and B. Koopmans, Control of speed and efficiency of ultrafast demagnetization by direct transfer of spin angular momentum, Nat. Phys. **4**, 855 (2008).

[4] M. Battiato, K. Carva, and P. M. Oppeneer, Superdiffusive Spin Transport as a Mechanism of Ultrafast Demagnetization, Phys. Rev. Lett. **105**, 027203 (2010).

[5] A. J. Schellekens, K. C. Kuiper, R. R. J. C. de Wit, and B. Koopmans, Ultrafast spin-transfer torque driven by femtosecond pulsed-laser excitation, Nat. Commun. **5**, 4333 (2014).

[6] J. Igarashi, Q. Remy, S. Iihama, G. Malinowski, M. Hehn, J. Gorchon, J. Hohlfeld, S. Fukami, H. Ohno, and S. Mangin, Engineering single-shot all-optical switching of ferromagnetic materials, Nano Lett. **20**, 8654 (2020).

[7] Y. L. W. van Hees, P. van de Meugheuvel, B. Koopmans, and R. Lavrijsen, Deterministic all-optical magnetization writing facilitated by non-local transfer of spin angular momentum, Nat. Commun. **11**, 3835 (2020).

[8] A. Melnikov, A. Povolotskiy, and U. Bovensiepen, Magnon-Enhanced Phonon Damping at Gd(0001) and Tb(0001) Surfaces Using Femtosecond Time-Resolved Optical Second-Harmonic Generation, Phys. Rev. Lett. **100**, 247401 (2008).

[9] D. Afanasiev, I. Razdolski, K. M. Skibinsky, D. Bolotin, S. V. Yagupov, M. B. Strugatsky, A. Kirilyuk, T. Rasing, and A. V. Kimel, Laser Excitation of Lattice-Driven Anharmonic Magnetization Dynamics in Dielectric $FeBO_3$, Phys. Rev. Lett. **112**, 147403 (2014).

[10] T. F. Nova, A. Cartella, A. Cantaluppi, M. Först, D. Bossini, R. V. Mikhaylovskiy, A. V. Kimel, R. Merlin, and A. Cavalleri, An effective magnetic field from optically drivenphonons, Nat. Phys. **13**, 132 (2017).

[11] S. F. Maehrlein, I. Radu, P. Maldonado, A. Paarmann, M. Gensch, A. M. Kalashnikova, R. V. Pisarev, M. Wolf, P. M. Oppeneer, J. Barker, and T. Kampfrath, Dissecting spin-phonon equilibration in ferrimagnetic insulators by ultrafast lattice excitation, Sci. Adv. **4**, eaar5164 (2018).

[12] C. Dornes, Y. Acremann, M. Savoini, M. Kubli, M. J. Neugebauer, E. Abreu, L. Huber, G. Lantz, C. A. F. Vaz, H. Lemke, E. M. Bothschafter, M. Porer, V. Esposito, L. Rettig, M. Buzzi, A. Alberca, Y. W. Windsor, P. Beaud, U. Staub, D. Zhu, S. Song, J. M. Glownia, and S. L. Johnson, The ultrafast Einstein–de Haas effect, Nature (London) **565**, 209 (2019).

[13] D.-L. Zhang, J. Zhu, T. Qu, D. M. Lattery, R. H. Victora, X. Wang, and J.-P. Wang, High-frequency magnetoacoustic resonance through strain-spin coupling in perpendicular magnetic multilayers, Sci. Adv. **6**, eabb4607 (2020).

[14] Y. W. Windsor, D. Zahn, R. Kamrla, J. Feldl, H. Seiler, C.-T. Chiang, M. Ramsteiner, W. Widdra, R. Ernstorfer, and L. Rettig, Exchange-Striction Driven Ultrafast Nonthermal Lattice Dynamics in NiO, Phys. Rev. Lett. **126**, 147202 (2021).

[15] S. R. Tauchert, M. Volkov, D. Ehberger, D. Kazenwadel, M. Evers, H. Lange, A. Donges, A. Book, W. Kreuzpaintner, U. Nowak, and P. Baum, Polarized phonons carry angular momentum in ultrafast demagnetization, Nature (London) **602**, 73 (2022).

[16] E. Y. Vedmedenko, R. K. Kawakami, D. D. Sheka, P. Gambardella, A. Kirilyuk, A. Hirohata, C. Binek, O. Chubykalo-Fesenko, S. Sanvito, B. J. Kirby, J. Grollier, K. Everschor-Sitte, T. Kampfrath, C.-Y. You, and A. Berger, The 2020 magnetism roadmap, J. Phys. D: Appl. Phys. **53**, 453001 (2020).

[17] G. E. W. Bauer, E. Saitoh, and B. J. van Wees, Spin caloritronics, Nature Mater. **11**, 391 (2012).

[18] T. Kampfrath, M. Battiato, P. Maldonado, G. Eilers, J. Nötzold, S. Mährlein, V. Zbarsky, F. Freimuth, Y. Mokrousov, S. Blügel,

M. Wolf, I. Radu, P. M. Oppeneer, and M. Münzenberg, Terahertz spin current pulses controlled by magnetic heterostructures, Nat. Nanotechnol. **8**, 256 (2013).

[19] J. B. Kortright, Resonant soft x-ray and extreme ultraviolet magnetic scattering in nanostructured magnetic materials: Fundamentals and directions, J. Electron Spectrosc. Relat. Phenom. **189**, 178 (2013).

[20] T. Sant, D. Ksenzov, F. Capotondi, E. Pedersoli, M. Manfredda, M. Kiskinova, H. Zabel, M. Kläui, J. Lüning, U. Pietsch, and C. Gutt, Measurements of ultrafast spin-profiles and spin-diffusion properties in the domain wall area at a metal/ferromagnetic film interface, Sci. Rep. **7**, 15064 (2017).

[21] V. Chardonnet, M. Hennes, R. Jarrier, R. Delaunay, N. Jaouen, M. Kuhlmann, N. Ekanayake, C. Léveillé, C. von Korff Schmising, D. Schick, K. Yao, X. Liu, G. S. Chiuzbăian, J. Lüning, B. Vodungbo, and E. Jal, Toward ultrafast magnetic depth profiling using time-resolved x-ray resonant magnetic reflectivity, Struct. Dyn. **8**, 034305 (2021).

[22] S. Macke and E. Goering, Magnetic reflectometry of heterostructures, J. Phys.: Condens. Matter **26**, 363201 (2014).

[23] M. Elzo, E. Jal, O. Bunau, S. Grenier, Y. Joly, A. Ramos, H. Tolentino, J. Tonnerre, and N. Jaouen, X-ray resonant magnetic reflectivity of stratified magnetic structures: Eigenwave formalism and application to a W/Fe/W trilayer, J. Magn. Magn. Mater. **324**, 105 (2012).

[24] B. Vodungbo, A. B. Sardinha, J. Gautier, G. Lambert, C. Valentin, M. Lozano, G. Iaquaniello, F. Delmotte, S. Sebban, J. Lüning, and P. Zeitoun, Polarization control of high order harmonics in the euv photon energy range, Opt. Express **19**, 4346 (2011).

[25] O. Kfir, P. Grychtol, E. Turgut, R. Knut, D. Zusin, D. Popmintchev, T. Popmintchev, H. Nembach, J. M. Shaw, A. Fleischer, H. Kapteyn, M. Murnane, and O. Cohen, Generation of bright phase-matched circularly-polarized extreme ultraviolet high harmonics, Nat. Photonics **9**, 99 (2015).

[26] T. Fan, P. Grychtol, R. Knut, C. Hernández-García, D. D. Hickstein, D. Zusin, C. Gentry, F. J. Dollar, C. A. Mancuso, C. W. Hogle, O. Kfir, D. Legut, K. Carva, J. L. Ellis, K. M. Dorney, C. Chen, O. G. Shpyrko, E. E. Fullerton, O. Cohen, P. M. Oppeneer, D. B. Milošević, A. Becker, A. A. Jaroń-Becker, T. Popmintchev, M. M. Murnane, and H. C. Kapteyn, Bright circularly polarized soft x-ray high harmonics for x-ray magnetic circular dichroism, Proc. Natl. Acad. Sci. USA **112**, 14206 (2015).

[27] G. Lambert, B. Vodungbo, J. Gautier, B. Mahieu, V. Malka, S. Sebban, P. Zeitoun, J. Luning, J. Perron, A. Andreev, S. Stremoukhov, F. Ardana-Lamas, A. Dax, C. P. Hauri, A. Sardinha, and M. Fajardo, Towards enabling femtosecond helicity-dependent spectroscopy with high-harmonic sources, Nat. Commun. **6**, 6167 (2015).

[28] S. Mathias, C. La-O-Vorakiat, P. Grychtol, P. Granitzka, E. Turgut, J. M. Shaw, R. Adam, H. T. Nembach, M. E. Siemens, S. Eich, C. M. Schneider, T. J. Silva, M. Aeschlimann, M. M. Murnane, and H. C. Kapteyn, Probing the timescale of the exchange interaction in a ferromagnetic alloy, Proc. Natl. Acad. Sci. USA **109**, 4792 (2012).

[29] M. Hofherr, S. Häuser, J. K. Dewhurst, P. Tengdin, S. Sakshath, H. T. Nembach, S. T. Weber, J. M. Shaw, T. J. Silva, H. C. Kapteyn, M. Cinchetti, B. Rethfeld, M. M. Murnane, D. Steil, B. Stadtmüller, S. Sharma, M. Aeschlimann, and S. Mathias, Ultrafast optically induced spin transfer in ferromagnetic alloys, Sci. Adv. **6**, eaay8717 (2020).

[30] P. Tengdin, C. Gentry, A. Blonsky, D. Zusin, M. Gerrity, L. Hellbrück, M. Hofherr, J. Shaw, Y. Kvashnin, E. K. Delczeg-Czirjak, M. Arora, H. Nembach, T. J. Silva, S. Mathias, M. Aeschlimann, H. C. Kapteyn, D. Thonig, K. Koumpouras, O. Eriksson, and M. M. Murnane, Direct light-induced spin transfer between different elements in a spintronic heusler material via femtosecond laser excitation, Sci. Adv. **6**, eaaz1100 (2020).

[31] F. Willems, C. von Korff Schmising, C. Strüber, D. Schick, D. W. Engel, J. K. Dewhurst, P. Elliott, S. Sharma, and S. Eisebitt, Optical inter-site spin transfer probed by energy and spin-resolved transient absorption spectroscopy, Nat. Commun. **11**, 871 (2020).

[32] S. Zayko, O. Kfir, M. Heigl, M. Lohmann, M. Sivis, M. Albrecht, and C. Ropers, Ultrafast high-harmonic nanoscopy of magnetization dynamics, Nat. Commun. **12**, 6337 (2021).

[33] F. Siegrist, J. A. Gessner, M. Ossiander, C. Denker, Y.-P. Chang, M. C. Schröder, A. Guggenmos, Y. Cui, J. Walowski, U. Martens, J. K. Dewhurst, U. Kleineberg, M. Münzenberg, S. Sharma, and M. Schultze, Light-wave dynamic control of magnetism, Nature (London) **571**, 240 (2019).

[34] C. D. Stanciu, F. Hansteen, A. V. Kimel, A. Kirilyuk, A. Tsukamoto, A. Itoh, and T. Rasing, All-Optical Magnetic Recording with Circularly Polarized Light, Phys. Rev. Lett. **99**, 047601 (2007).

[35] I. Radu, K. Vahaplar, C. Stamm, T. Kachel, N. Pontius, H. A. Dürr, T. A. Ostler, J. Barker, R. F. L. Evans, R. W. Chantrell, A. Tsukamoto, A. Itoh, A. Kirilyuk, T. Rasing, and A. V. Kimel, Transient ferromagnetic-like state mediating ultrafast reversal of antiferromagnetically coupled spins, Nature (London) **472**, 205 (2011).

[36] D. Céspedes-Berrocal, H. Damas, S. Petit-Watelot, D. Maccariello, P. Tang, A. Arriola-Córdova, P. Vallobra, Y. Xu, J.-L. Bello, E. Martin, S. Migot, J. Ghanbaja, S. Zhang, M. Hehn, S. Mangin, C. Panagopoulos, V. Cros, A. Fert, and J.-C. Rojas-Sánchez, Current-induced spin torques on single GdFeCo magnetic layers, Adv. Mater. **33**, 2007047 (2021).

[37] S. Krishnia, E. Haltz, L. Berges, L. Aballe, M. Foerster, L. Bocher, R. Weil, A. Thiaville, J. a. Sampaio, and A. Mougin, Spin-Orbit Coupling in Single-Layer Ferrimagnets: Direct Observation of Spin-Orbit Torques and Chiral Spin Textures, Phys. Rev. Appl. **16**, 024040 (2021).

[38] M. van Mörbeck-Bock, T. Feng, A. Heilmann, L. Ehrentraut, H. Stiel, M. Hennecke, T. Sidiropoulos, C. von Korff Schmising, S. Eisebitt, and M. Schnürer, High average power OPCPA MIR-systems for coherent soft x-ray generation accessing absorption edges of metals, in *High Power Lasers and Applications*, edited by J. Hein, T. J. Butcher, P. Bakule, C. L. Haefner, G. Korn, and L. O. Silva (International Society for Optics and Photonics, Bellingham, WA, 2021), Vol. 11777, pp. 11–16.

[39] See Supplemental Material at http://link.aps.org/supplemental/10.1103/PhysRevResearch.4.L022062 for more details about the TMOKE measurements, simulations, hard x-ray reflectometry, and pump pulse absorption.

[40] T. A. Ostler, R. F. L. Evans, R. W. Chantrell, U. Atxitia, O. Chubykalo-Fesenko, I. Radu, R. Abrudan, F. Radu, A. Tsukamoto, A. Itoh, A. Kirilyuk, T. Rasing, and A. Kimel,

Crystallographically amorphous ferrimagnetic alloys: Comparing a localized atomistic spin model with experiments, Phys. Rev. B **84**, 024407 (2011).

[41] D. Schick, UDKM1DSIM–a Python toolbox for simulating 1D ultrafast dynamics in condensed matter, Comput. Phys. Commun. **266**, 108031 (2021).

[42] M. Wietstruk, A. Melnikov, C. Stamm, T. Kachel, N. Pontius, M. Sultan, C. Gahl, M. Weinelt, H. A. Dürr, and U. Bovensiepen, Hot-Electron-Driven Enhancement of Spin-Lattice Coupling in Gd and Tb $4f$ Ferromagnets Observed by Femtosecond X-Ray Magnetic Circular Dichroism, Phys. Rev. Lett. **106**, 127401 (2011).

[43] L. Rettig, C. Dornes, N. Thielemann-Kühn, N. Pontius, H. Zabel, D. L. Schlagel, T. A. Lograsso, M. Chollet, A. Robert, M. Sikorski, S. Song, J. M. Glownia, C. Schüßler-Langeheine, S. L. Johnson, and U. Staub, Itinerant and Localized Magnetization Dynamics in Antiferromagnetic Ho, Phys. Rev. Lett. **116**, 257202 (2016).

[44] B. Koopmans, G. Malinowski, F. Dalla Longa, D. Steiauf, M. Fähnle, T. Roth, M. Cinchetti, and M. Aeschlimann, Explaining the paradoxical diversity of ultrafast laser-induced demagnetization, Nature Mater. **9**, 259 (2010).

[45] M. Battiato, K. Carva, and P. M. Oppeneer, Theory of laser-induced ultrafast superdiffusive spin transport in layered heterostructures, Phys. Rev. B **86**, 024404 (2012).

[46] A. Eschenlohr, M. Battiato, P. Maldonado, N. Pontius, T. Kachel, K. Holldack, R. Mitzner, A. Föhlisch, P. M. Oppeneer, and C. Stamm, Ultrafast spin transport as key to femtosecond demagnetization, Nature Mater. **12**, 332 (2013).

[47] A. Slachter, F. L. Bakker, J.-P. Adam, and B. J. van Wees, Thermally driven spin injection from a ferromagnet into a nonmagnetic metal, Nat. Phys. **6**, 879 (2010).

[48] G.-M. Choi, B.-C. Min, K.-J. Lee, and D. G. Cahill, Spin current generated by thermally driven ultrafast demagnetization, Nat. Commun. **5**, 4334 (2014).